# 18B.2 Mesoscale Modelling for Radar Propagation Prediction during the Wallops-2000 Experiment

Changgui Wang*(1), Peter A Clark (1), Tracy Haack (2), Sarah Millington (1)

(1) Met Office, Exeter, United Kingdom
(2) The Naval Research Laboratory, Monterey, CA, USA

## Abstract

In coastal regions, advection of an air mass from the land over the water may result in a large change in temperature and humidity which has a significant impact on the occurrence of radar ducting. Radar ducting occurs when modified refractive index decreases with height where sharp changes in humidity and temperature appear. Understanding the changes of radar propagation conditions in such complicated coastal environments is vital to national defence agencies around the world and thus requires an ability to predict the evolution of atmospheric refractivity in time and space. To this end, this study aims to assess the feasibility of using a high resolution Numerical Weather Prediction (NWP) model to predict duct existence, height and intensity in relation to synoptic and local weather features. The NWP model used here is the Met Office Unified model (MetUM) running with grid lengths of 12km, 4km and 1.5km. Hourly model results were then evaluated and assessed against field measurements (Wallops-2000 experiment) collected over 7-day intensive observations between 28 April and 4 May 2000 near Wallops Island off the shores of Virginia, USA. The Wallops-2000 experiment was made available through the collaboration between ABCANZ countries (America, Britain, Canada, Australia and New Zealand).

This study focuses on the verification of near-shore and over-water surface and boundary layer temperature and moisture and ducting characteristics. The model predictions are compared and evaluated with buoy, helicopter measurements in terms of time-series and vertical profiles. The characteristics of ducts occurring at the locations of helicopter profiles were also examined statistically, indicating a high occurrence rate of surface ducts. The model time-height profile at the Naval Postgraduate Student buoy site shows that surface ducts occur during the whole experiment period with different degree of strength. Strong and thick surface ducts were also found in both observations and model results at the shallow marine boundary layer (MBL) while the most elevated ducts were only predicted at the deep MBL where observations were not available. The high resolution NWP model exhibits its ability to capture these trends and characteristics in the ducting trapping layer as compared with the measurements. These statistics are discussed in association with local meteorological conditions and weather systems affecting the region.

* *Corresponding author address*: Changgui Wang, JCMM, Met Office, Reading, RG6 6BB, United Kingdom; email: chang.wang@metoffice.gov.uk

# 1. Introduction

Synoptic weather and local meteorological conditions have a significant impact on the occurrence, height and intensity of ducts which affect the propagation path of radar signals through the atmosphere, especially in the atmospheric boundary layer over ocean and coastal areas. They are responsible for vertical variations of temperature; humidity and pressure which in turn alter the radar energy propagate through the atmosphere. A rapid variation in these profiles can cause the formation of ducts. Anomalous variations in vertical temperature and humidity gradients that yield a negative gradient of modified refractive index indicate the presence of ducting conditions. Such refractive effects are of particular importance to strike warfare, ship self-defence and special operations. The modified refractivity M is defined by

$$M=\frac{77.6}{T}(p+4810\frac{e}{T})+\frac{z}{R}*10^{6}$$

in which *T* is the air temperature in Kelvin; *p* is the air pressure in hPa; *e* is the water vapour pressure in hPa; *z* is the height above sea level and *R* is the mean radius of the earth. For a spherical earth with an atmosphere having a uniform refractive index, rays are curved relative to the earth. This is approximately equivalent to a flat earth with an atmosphere in which the refractive index varies with height. If refractivity (*M*) decreases with height, then the radar beam could be trapped in a duct.

In coastal regions, advection of an air mass from the land over the water may result in a large change in temperature and humidity. When warm, dry continental air travels over cooler water, it increases stability and suppresses vertical mixing. Heat loss to the surface results in the cooling of the air nearest the surface and forms a stable internal boundary layer (IBL) within the existing boundary layer. As a result, moisture evaporated from the sea is trapped within the shallow IBL and leads to the formation of a duct. Understanding the changes of radar propagation conditions in such complicated coastal environments requires an ability to predict the evolution of atmospheric refractivity in time and space. To this end, this study aims to assess the feasibility of using the high resolution Numerical Weather Prediction (NWP) models to predict duct existence, height and intensity in relation to synoptic and local weather features. Model results were evaluated and assessed using the complete dataset from the Wallops-2000 Experiment conducted at Wallops Island, VA, USA which made available through the collaboration between ABCANZ countries (America, Britain, Canada, Australia and New Zealand). The experiment was carried out mainly to evaluate surface ducting features. Measurements in the trial included low-elevation radar frequency pathloss and clutter returns as well as meteorological conditions from a Met Tower (over land), buoys and helicopter path profiles for a entire week period from 28th April to 4th May 2000. An extensive description of the field campaign and observations gathered during the field experiment were presented by Stapleton *et al* (2001) and Burk and Haack (2003).

This paper focuses on the verification of near-shore and over-water surface and boundary layer temperature and moisture and ducting characteristics. The 4km and 1.5 km model predictions were compared and evaluated with buoy, helicopter measurements as shown in Figure 1 in terms of time-series and vertical profile statistics. In addition, the characteristics of daily duct occurrence at the observation locations were also examined in association with the local meteorological conditions and weather systems affecting the region

.

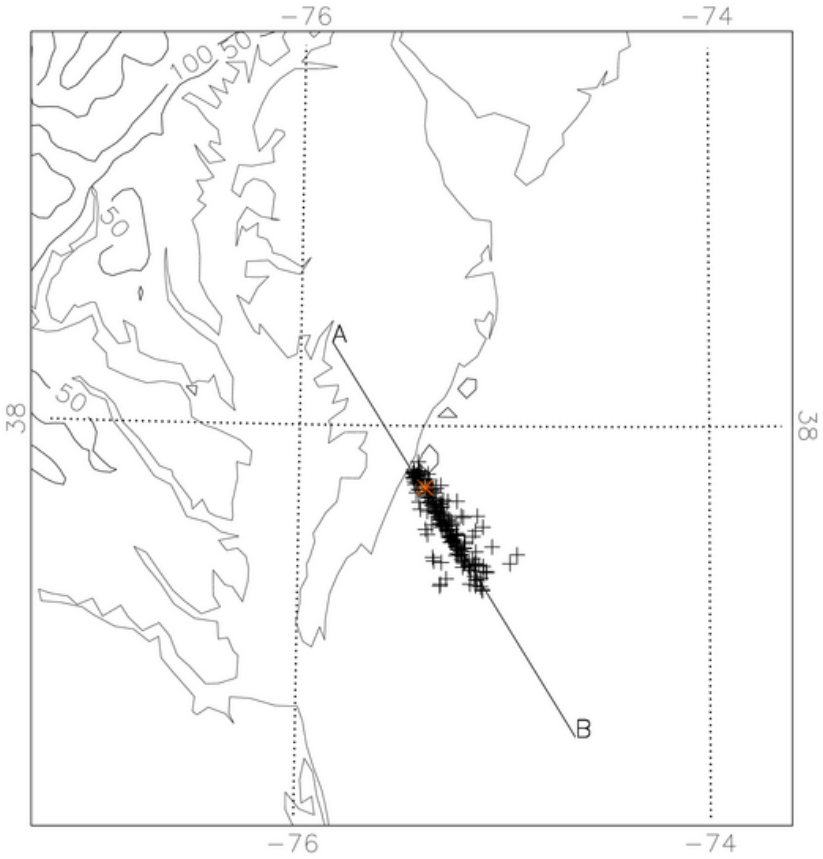


**Figure 1** the location of NPS buoy and the coverage of helicopter measurements during the Wallops-2000 experiment. The signs of red '*' and black '+' indicate the NPS and helicopter locations.

## 2. NWP Model and Setup

The mesoscale topography of this coastal region and strong sea surface temperature gradients between cool shelf waters and the warm Gulf Stream produce complex boundary layer (BL) structures that often generate distinct vertical refractivity gradients and alter electromagnetic (EM) propagation. To analyze and forecast refractivity variations affected by complex BL structures in the region, the Met Office Unified Model (MetUM) with high horizontal and vertical resolution was used in this study.

The dynamic core of this model implements the fully compressible, non-hydrostatic, deep atmosphere formulation of the Navier-Stokes equations and its details were described by Davies *et al* (2005). The model includes a comprehensive set of parameterizations, including surface (Essery, *et al.* 2001), boundary layer (Lock *et al.* 2000), mixed phase cloud microphysics (Wilson and Ballard 1999) and convection (Gregory and Rowntree (1990), with additional downdraft and momentum transport parameterizations). The model runs on a rotated latitude/longitude horizontal grid with Arakawa C staggering and, a terrain-following hybrid-height vertical coordinate with Charney-Philips staggering. As the model is non-hydrostatic, it is appropriate to be run at a high horizontal resolution (e.g. 4 km and 1.5 km) which will preserve the important features of the topography and coastline that can impact strongly on the formation of radar holes and ducts.

For this study, a suite of (one way) nested models (Figure 2) were setup to reconfigure and run with grid lengths of 12km, 4km and 1.5km respectively. The 12km Model was run for 24 hours in the way of dynamical adaptation downscaled analysis using the global analyses (horizontal resolution: 0.5°x0.5°, 60 level) from ECMWF (European Centre for Medium-Range Weather Forecasts) starting at 00Z for each day to provide boundaries for the 4km model whilst the boundaries for the 1.5km model were derived from the 4km model. Initial conditions for all models were interpolated from the ECMWF global analysis. The detailed model configuration is listed in Table 1.

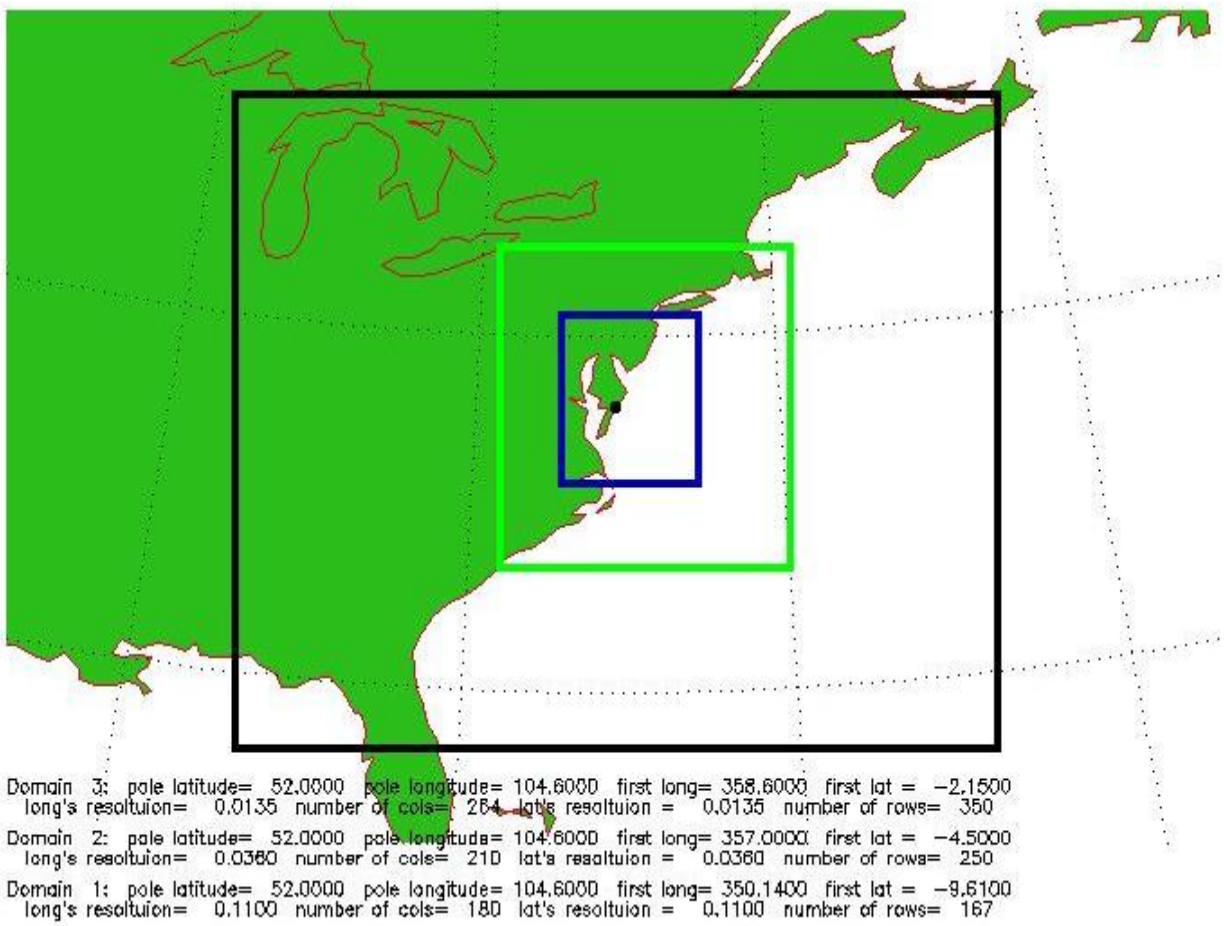


**Figure 2. Wallops Island model domains**

**Table 1** MetUM configurations

| | **12km** | **4km** | **1.5km** |
|---|---|---|---|
| Number of levels | 38 | 70 | 70 |
| Top of model (m) | approx. 40000 | approx. 40000 | approx. 40000 |
| Number of ozone levels | 11 | 35 | 35 |
| Driving model | ECMWF global dynamic adaptation and downscaled analysis | 12km Downscaled forecast | 4km Downscaled forecast |
| Rimwidth | 8 | 8 | 8 |
| Time frequency | 180 min | 30 min | 15 min |
| Model timestep | 5 mins | 100s | 30s |
| Radiation timestep | 60 min | 15 min | 5 min |
| Convection scheme | Mass flux with CAPE closure timescale 1800s | Mass flux CAPE dependent CAPE closure timescale 1200s | No convection scheme |
| Microphysics | Dual phase including iterative melting. | Dual phase with prognostic rain. | Dual phase with prognostic rain. |
| Gravity Wave Drag | On | Off | Off |
| Boundary Layer | 13 levels | 30 levels | 30 levels |

# 3. NWP Model Outputs and Analysis

The nested high-resolution MetUM mesoscale models described above were run 24 hours starting at 00Z each day and the hourly outputs were produced for the whole period of the Wallops-2000 field experiment. The sea surface temperature (SST) in the 4km model was updated using the NCODA SST and then interpolated onto the 1.5km model domain. The 4km and 1.5km model outputs of temperature, humidity, winds, modified refractivity and ducting characteristics were assessed against the measurements at NPS and helicopter paths.

## *MetUM modelling results versus verifying measurements*

Figure 3 and Figure 4 shows the full week time-series from both models at the NPS buoy located about 12km offshore of Wallops Island, the MetUM forecasts of temperature, relatively humidity, wind speed and direction are in red and observations in black. The comparison of time-series statistics of the model results and measurements indicates that the both model results have a very good agreement with the observations at the NPS buoy. The 4km model (Figure 3) shows the RMSE errors of 0.87K for temperature, 6.52% for RH, 1.52 m/s and 53.13 degree for wind speed and wind direction. The 1.5km model (Figure 4) shows very similar RMSE but slightly higher bias with an exception of better winds predicted. In particular both models demonstrated their ability to predict the very dry air with high temperature around 21Z on the 30$^{th}$ April 2000. Figure 3 and Figure 4 also show temperature spikes at 00Z on 29$^{th}$, 30$^{th}$ April and 2$^{nd}$ May 2000 which were not observed at the NPS. As these spikes occurred at the 00Z, therefore, it is suspected that this is due to the transition of the model runs from one day to another. The high RMSE and bias of wind directions were also

due to the model results staged a couple of hours from 00Z on 1st and 3rd May. The behaviour of both temperature and wind directions was caused by interpolation artefact and suggest that model forecast sinning up at first few hours, say 3-6 hours, should not be used with high resolution models.

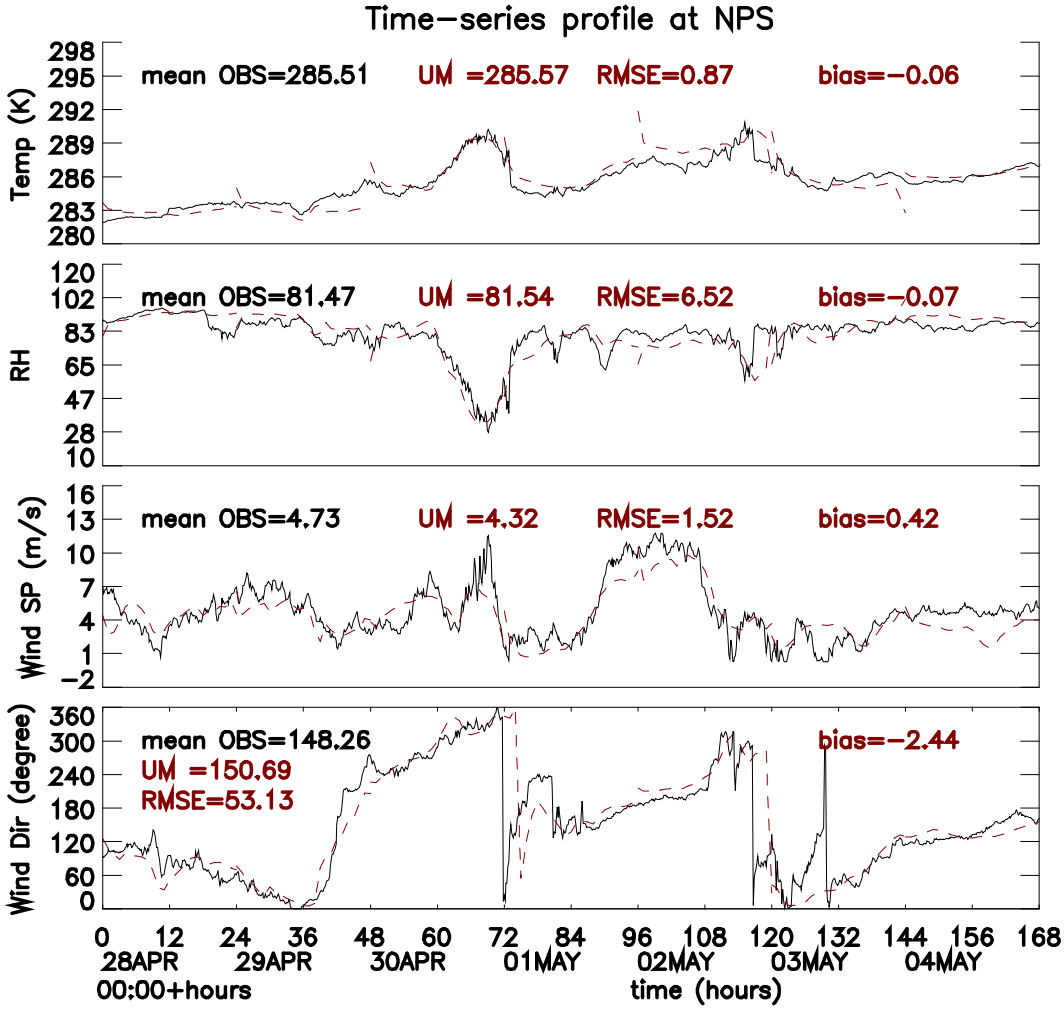


**Figure 3** The 4km model time-series against observations at the NPS. Model forecasts are in red and the observations in black.

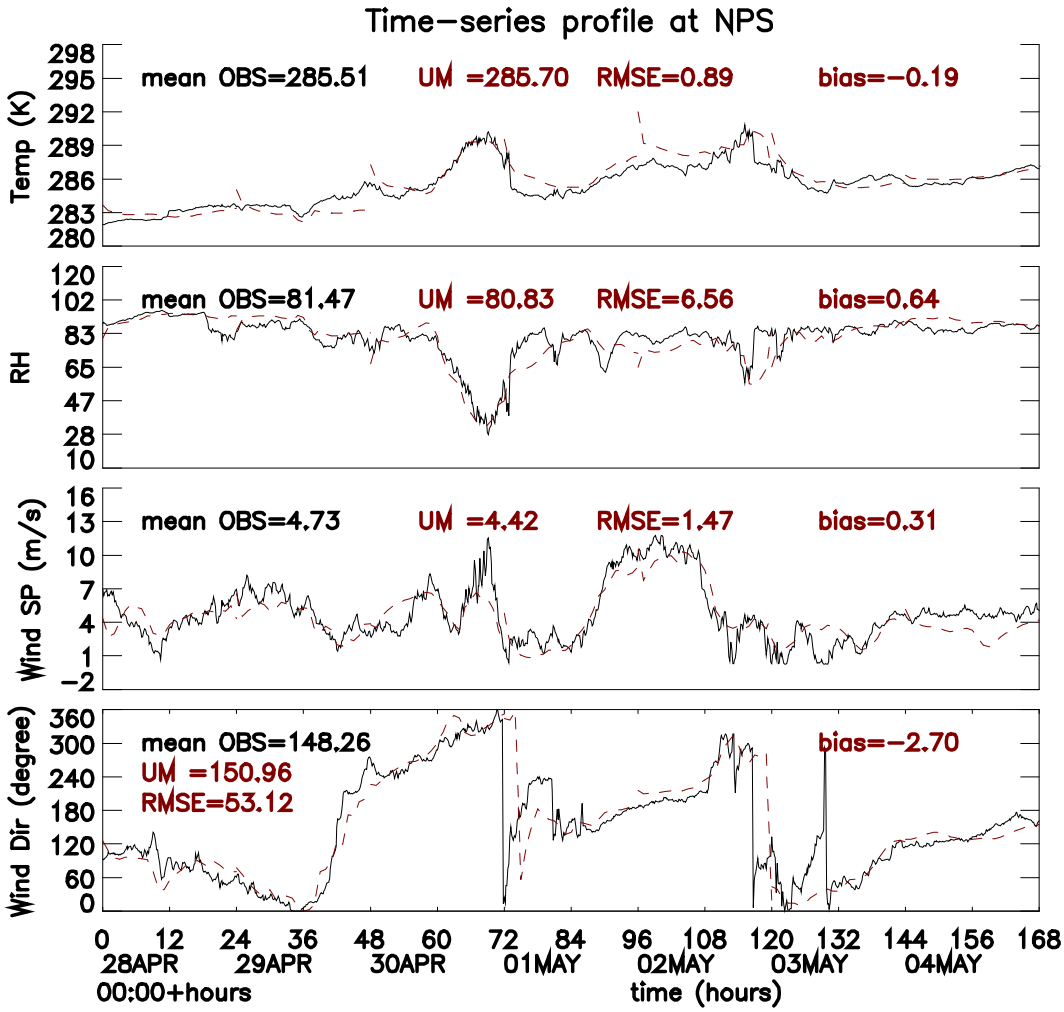


**Figure 4** the 1.5km model time-series against observations at the NPS. Model forecasts are in red and the observations in black.

The model results were also compared with the helicopter vertical measurements. The vertical profiles were derived hourly at vertically averaged locations from near hour helicopter observations. The resulting statistics for potential temperature, specific humidity and modified refractivity together with corresponding observations are listed in Table 2. The predicted specific humidity from the both models showed a very good agreement with helicopter measurements, in particular at the near surface. The best match was at the first model level of 5m with the bias of only -0.01q/kg and its RMSE is 0.64g/kg. In contrast, the potential temperature was under-forecast from both models and showed a disagreement with the observations with the model bias reaching to -1.6K. However, it is observable from the first five level's statistics that the variation in the model bias and RMSE for the potential temperature was very small. Figure 5 depicts one of vertical profiles validated at 16Z on 4$^{th}$ May 2000 and it shows that the shape of the model temperature profile is broadly consistent with the observation profile apart from that slightly sharper gradient occurred at a level of about 65m. This finding suggests that a further examination on the measured temperature may be necessary.

Table 2 Vertical profile statistics at Helicopter paths: bias = model mean-obs mean

| Ht (m) | Num. of points | **Obs-mean** | **4km mean** | 4km bias | 4km RMSE | **1.5km mean** | 1.5km bias | 1.5km RMSE |
|---|---|---|---|---|---|---|---|---|
| **Specific humidity** | | | | | | | | |
| 112 | 189 | **5.85** | **5.97** | 0.12 | 1.14 | **6.00** | 0.14 | 1.12 |
| 75 | 190 | **6.09** | **6.24** | 0.15 | 1.22 | **6.09** | 0.17 | 1.19 |
| 45 | 190 | **6.60** | **6.65** | 0.05 | 0.99 | **6.60** | 0.04 | 0.96 |
| 22 | 190 | **6.95** | **6.94** | -0.01 | 0.67 | **6.95** | -0.02 | 0.66 |
| 5 | 190 | **7.19** | **7.19** | -0.01 | 0.64 | **7.19** | -0.01 | 0.53 |
| **Potential temperature** | | | | | | | | |
| 112 | 189 | **288.34** | **286.76** | -1.59 | 1.85 | **388.35** | -1.62 | 1.86 |
| 75 | 190 | **287.82** | **286.06** | -1.75 | 1.90 | **287.82** | -1.77 | 1.89 |
| 45 | 190 | **286.97** | **285.24** | -1.72 | 1.91 | **286.97** | -1.70 | 1.88 |
| 22 | 190 | **286.25** | **284.63** | -1.62 | 1.79 | **286.25** | -1.60 | 1.80 |
| 5 | 190 | **285.72** | **284.08** | -1.64 | 1.94 | **285.79** | -1.67 | 1.86 |
| **Modified Refractivity** | | | | | | | | |
| 112 | 189 | **330.14** | **333.55** | 3.41 | 8.87 | **333.72** | 3.58 | 8.69 |
| 75 | 190 | **327.61** | **331.45** | 3.83 | 9.67 | **331.58** | 3.96 | 9.36 |
| 45 | 190 | **328.45** | **331.52** | 3.07 | 7.97 | **331.40** | 2.94 | 7.65 |
| 22 | 190 | **328.91** | **331.39** | 2.48 | 5.42 | **331.30** | 2.39 | 5.30 |
| 5 | 190 | **329.19** | **331.64** | 2.44 | 4.91 | **331.54** | 2.37 | 4.45 |

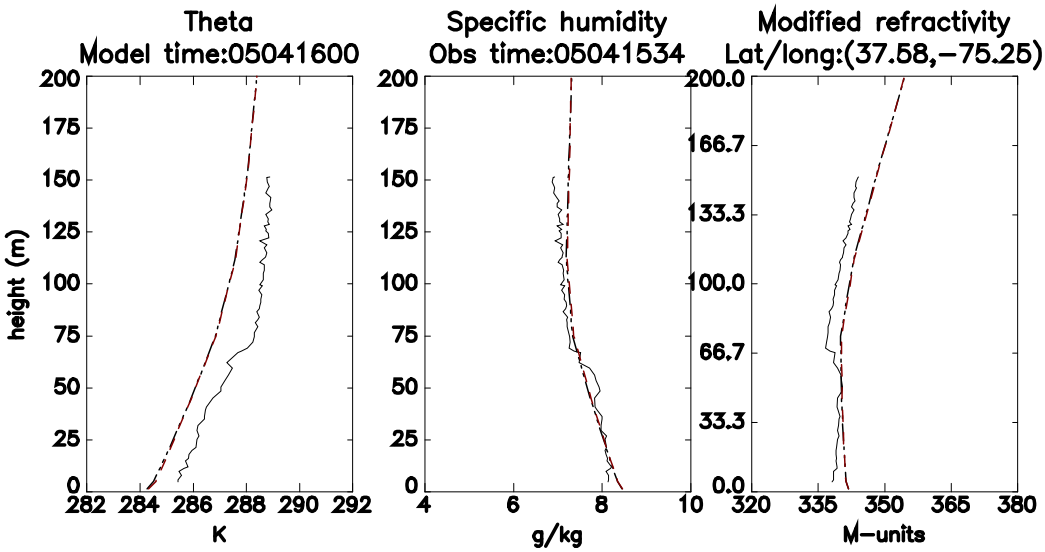


**Figure 5** Vertical profiles at 16:00Z on 4/5/2000 at one of helicopter measurement locations. Solid line is observations; Overlapped dashed and dot-dashed lines are for 4km and 1.5km models.

The MetUM forecast performance for radar propagation conditions were examined against a total of 190 helicopter vertical measurements. Table 3 presents a ducting contingency table (Panofsky and Brier, 1958) for observed and predicted cases of ducting and no-ducting. Table 4 illustrates ducting properties detected by both the MetUM models and the measurements and Figure 6 demonstrates forecast skills of both models. With duct events of 110 and 113 for the 4km model and 1.5km model respectively, Table 4 shows that MetUM under-predicted duct strength and base height but over-predicted duct thickness as shown in Figure 5. The 1.5km MetUM predicted even slightly less strength and thicker with a total of 113 duct events but the difference between the 4km and 1.5km models is not obvious from the helicopter vertical path profiles, Table 2 shows very little difference in the overall mean value of modified refractivity and one of vertical profiles as show in Figure 5 proved no distinction difference between the 4km and 1.5km model. The tendency of predicting weaker and thicker ducts was a consequence of less sharpness of gradient in specific humidity as well as the marine temperature inversion as shown in Figure 5 across IBL top at the height of about 65m.

**Table 3** Ducting contingency table from each model forecast:

| Ducting events | | 4km | | 1.5km | | Total | Comments |
|---|---|---|---|---|---|---|---|
| | | Yes | No | Yes | No | | *A*: event of "ducting"<br>*Y*: event of "no ducting"<br>*B*: the number of ducting found in the observation but not forecasted in the model;<br>*X:* is the number of ducting forecast in the model but not found in the observations. |
| Observation | Yes | 110 *(A)* | 23 *(B)* | 113 *(A)* | 20 *(B)* | 133 | |
| | No | 23 *(X)* | 34 *(Y)* | 23 *(X)* | 34 *(Y)* | 57 | |
| Total | | 133 | 57 | 136 | 54 | 190 | |

**Table 4** Ducting statistics at helicopter paths ('+' in Figure 1) computed from each model forecast where ducting observed from helicopter measurements.

| **Ducting properties** | **4km** (110 duct events) | | | **1.5km** (113 duct events) | | |
|---|---|---|---|---|---|---|
| | **mean** | **bias** | **RMSE** | **mean** | **bias** | **RMSE** |
| Base height (m) | 0.50 | 0.001 | 5.27 | 0.38 | -0.10 | 5.27 |
| Strength (M-units) | 5.13 | -2.25 | 7.28 | 4.54 | -3.12 | 7.34 |
| Thickness (m) | 71.17 | 6.60 | 43.76 | 69.78 | 3.23 | 46.52 |

The forecast skills of both models are depicted in Figure 6. It shows that the correct forecast rate (CFR) in which both duct events and no duct events are predicted correctly is ~76% for the 4km model and 77% for the 1.5km model. Ducting hit rates are 83% and 85% for the 4km and 1.5km models respectively. However, in a total of 57 observed no-duct events, 23 of them were forecasted as duct events, thus the correct null forecast rate was 60% for both models. With a total of 190 observations, the forecast errors were 24% and 23% for the 4km and 1.5km model corresponding. Considering the approximation of deriving the model vertical

profiles and the fact that the MetUM was set up to run with downscaling the ECMWF global analysis without any further data assimilation, the forecast skills from both 4km and 1.5km models demonstrated the MetUM's capability of correctly predicting the radar propagation conditions.

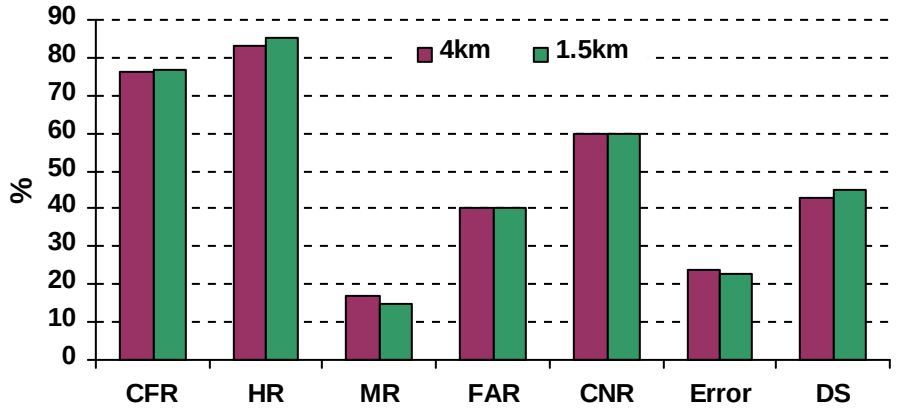


**Figure 6** Ducting forecasting skills from each model calculated from the contingency Table 3: *N = A+B+X+Y*; CFR (correct forecast rate) = *(A+Y)/N*; HR (hit rate) = *A/(A+B)*; MR (miss rate) = *B/(A+B)*; FAR (false alarm rate) = *X/(X+Y)*; CNR (correct null rate) = *Y/(X+Y)*; DS (discrimination score) = *A/(A+B)-X/(X+Y); Error=(X+B)/N*

## *Formation of ducts versus the synoptic and local weather conditions*

Synoptic and local weather conditions changed dramatically during the Wallops-2000 experiment. From 28th April, a low pressure system was moving from the South-west towards North-east of the Wallops Island. By 1st May, the low drifted away from the model domain and a high formed following this low. The 2nd May was affected by this high first and then a low from the North-east of Wallops Island. Behind this low, another high was developing from the North and then settled at the North-east of Wallops Island for the rest of the experiment period.

Figure 7 shows the time-height profiles of specific humidity, potential temperature, modified refractivity together with the ducting layer and wind vectors at the NPS buoy site. Figure 7 (a) and (b) are derived from the 4km and 1.5km modes respectively and both model captured the same structure and characteristics of the ducts. It is evident that the local weather and the formation of the ducts near the Wallops Island were mainly driven by the local thermal contrast and synoptic weather conditions. Along with the change of synoptic and local weather conditions over and near Wallops Island, onshore flow on 28th was backed to the North-east, North on 29th, and then the West on 30th April. As a result, the gradient of water vapour was getting sharper due to more dry air advection from the land. Therefore, the model picked up the surface ducts gradually from 29th April and the ducting layer became stronger and thicker.

As the low moving toward the east boundary of the domain, the winds veered to the North-west and then stronger Northerly winds by the end of 30th April. The advection of dry air from the land over the sea together with the subsidence led to the development of a more stable IBL. Hence the ducting layer was growing stronger and thicker. A column of very dry air (red) occurred at 21Z on 30th April as shown in Figure 7 which was confirmed with the observation at the NPS buoy (Figure 3).

On the 2nd May, strong South-west winds over Wallops were the combined effects of the low pressure at North and high pressure at the South-east of the Wallops. Consequently, the air changed from very dry to very moist and ducting layer was getting weaker and thinner on this day. As the low was moving South-eastwards, the high pressure system developed at the North of Wallops. Thus, the North-east and East winds on the 3rd May introduced dry air from the North into the region and changed the gradient of the water vapour again, so did the ducting structure. On the 4th May, the winds changed to the East and then the South-east, so the ducting formation altered to have elevated ducts due to the sea-breeze circulation as well as the surface ducts.

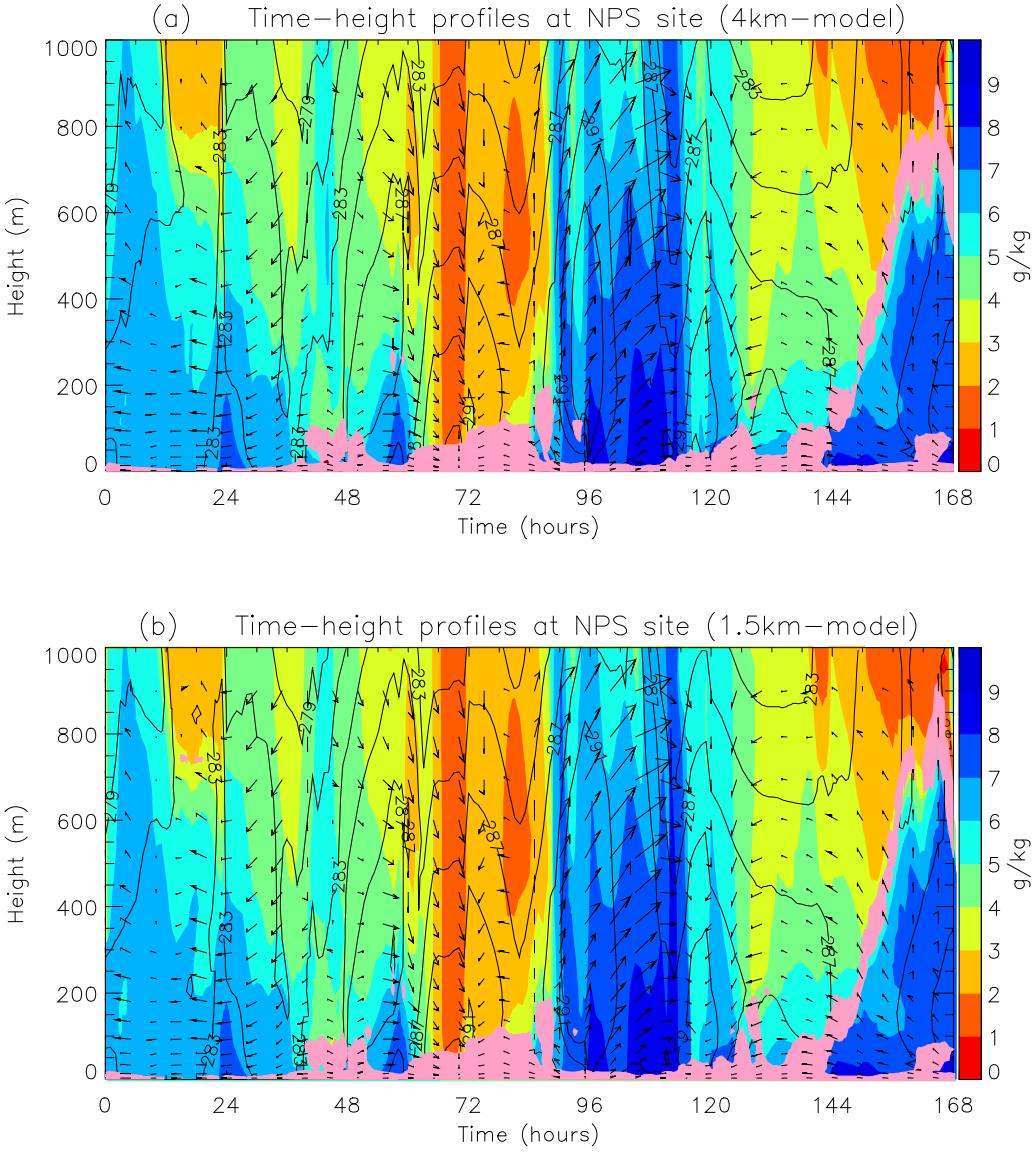


**Figure 7** time-height vertical profiles from both the 4km and 1.5km models. Colour shaded image is water vapour; contours are potential temperature; Pink colour indicates ducting layer; arrows are horizontal wind vectors (westerly and southerly winds).

## *Modelled daily and surface ducting events against measurements*

The formation of trapping layer occurred throughout the experiment period except 28th April 2000 which was evident from the daily event analysis of helicopter vertical profiles as shown in Figure 8. The time-high profile depicted above (Figure 7) clearly shows that the MetUM forecast the existence and the general structure of the trapping layer when compared with daily duct properties of the helicopter measurements. The daily event analysis in Figure 8 indicates that 28th April was the only day which was free of ducts predicted by both observation and the models.

For the rest of days during the experiment both models perform quite well despite the models over-predicting ducts of the event on 29th April and under-predicting on 3rd May. On the 29th April both models forecasted the same ducting event frequency. However, the 1.5km model was in closer agreement with the observation than the 4km model for the 3rd May. With predicted ducting events (133 in the 4km and 136 in the 1.5km model), both models predicted 95% of the surface ducting events which was higher than the observed surface duct of 90% (out of 133 observed ducts).

To examine diurnal ducting variations, Table 5 presents the daily diurnal changes of ducting strength, base height and thickness at the NPS buoy from the 4km model. It is evident that ducts in the afternoon were stronger than those in the morning except on 1st May when subsidence occurred, driven by the synoptic weather conditions (a high pressure system). The ducting thickness varied from day to day although afternoon ducts were slightly thicker than the morning ducts with the exception on 1st May. The ducts on most days were also featuring surface ducts apart from that elevated ducts occurred on 4th May. The strongest duct occurred on 30th April in the afternoon which reached to 13 M-units which was caused by the subsidence of the high pressure system.

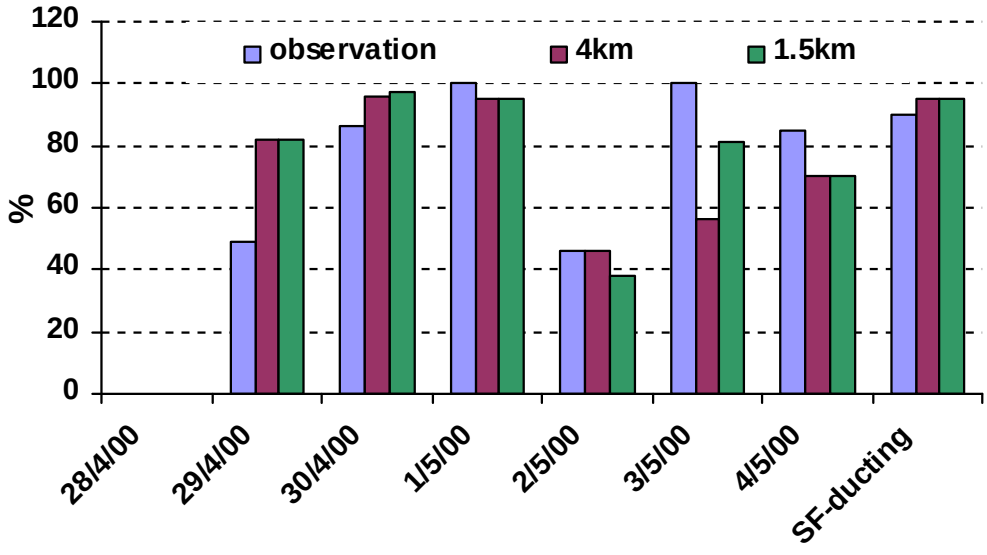


**Figure 8** Daily ducting events and the surface ducting (SF-ducting) frequency from each model forecast

**Table 5 surface duct frequency=80%. Am: 9:00-16Z; pm: 17:00-24Z; -999 stands for missing value or no-duct event**

| Date | Frequency | Strength (M-uints) | thickness | Base |
|---|---|---|---|---|
| 28/04/00 (am) | 0.00000 | -999.000 | -999.000 | -999.000 |
| 28/04/00 (pm) | 0.00000 | -999.000 | -999.000 | -999.000 |
| 29/04/00 (am) | 0.428571 | 1.33333 | 39.0000 | 0.00000 |
| 29/04/00 (pm) | 1.00000 | 7.37500 | 67.0000 | 0.00000 |
| 30/04/00 (am) | 0.571429 | 7.00000 | 39.0000 | 0.00000 |
| 30/04/00 (pm) | 1.00000 | 12.6250 | 48.7500 | 0.00000 |
| 01/05/00 (am) | 0.142857 | 9.14286 | 105.00000 | 0.00000 |
| 01/05/00 (pm) | 0.125000 | 1.00000 | 5.00000 | 0.00000 |
| 02/05/00 (am) | 1.00000 | 2.00000 | 21.0000 | 0.00000 |
| 02/05/00 (pm) | 1.00000 | 5.25000 | 25.0000 | 0.00000 |
| 03/05/00 (am) | 1.00000 | 1.14286 | 28.7143 | 0.00000 |
| 03/05/00 (pm) | 1.00000 | 6.87500 | 94.0000 | 0.00000 |
| 04/05/00 (am) | 0.857143 | 3.16667 | 253.833 | 364.000 |
| 04/05/00 (pm) | 1.00000 | 6.87500 | 305.375 | 366.125 |

# 4. Summary and conclusion

Two high resolution NWP models have been utilised to forecast the atmospheric conditions and the modified refractivity over the Atlantic shelf near Wallops Island and results were evaluated using observation data sets from the NPS buoy and helicopter profiles. Both 4km and 1.5km models predicted the presence of ducts with over 80% of hit rate near Wallops Island during the period of Wallops-2000 experiment. The results from these models confirm that duct trapping layers formed due to the subsidence and the formation of stable IBL with the following characteristics:

- Dry and warm air advecting over cooler water created stable IBLs that have the potential to form a trapping layer. However, the humidity gradients must be strong in order for a trapping layer to form. 30$^{th}$ April and 1$^{st}$ May 2000 were two examples to show that both models captured the effect of subsidence on the formation of ducting.

- Both the 4km and 1.5km models produced very similar results with fine ducting layers covering wide areas. However, the 1.5km model does not seem to perform better than the 4km model for this case when compared with observations. This could be the effects of the topography, particular synoptic conditions during the experiment period and the use of coarse resolution global data which some surface fields are from climatology and may not be a good choice for very high resolution models. Therefore, further work is required to verify the 1.5km model with different synoptic conditions as well as different surface conditions.

The NWP approach has a great advantage of providing 3-Dimensional information for the analysis and forecast of refractive conditions. This study demonstrates the potential of the NWP high-resolution models (4km and 1.5km) for providing such additional information for radar propagation forecast on the fine spatial and temporal characteristics of radar ducts. However, further investigation is needed to whether the 4km model is good enough to forecast reliable radar propagation or a higher resolution of 1.5km is required; in particular the validation of:

- Higher vertical resolution to represent more accurate vertical gradients of temperature, specific humidity and modified refractivity
- Impact of BL stability functions, BL structure in coastal transition with or without land and sea breeze
- The impact of BL scheme itself whether a higher order scheme is needed
- Consideration of model spin-up time.

***Acknowledgments****:* The authors are grateful to the UK Ministry of Defence for financial support of this research project. We also thank Damian Wilson and Humphrey Lean for their support.

## *REFERENCES*

Burk, S.D., T. Haack, L.T. Rogers, and L.J. Wagner, 2003: Island wake dynamics and wake influence on the evaporation duct and radar propagation. *J. Appl. Meteor.*, **42**, 349-367.

Davies, T, Cullen, M.J.P., Malcolm A.J., Mawson M.H., Staniforth, A., White, A.A. and Wood, N. 2005; A new dynamical core for the Met Office's global and regional modelling of the atmosphere. Q J R. Meteorol. Soc. **131** 1759-1782.

Essery, R. , Best, M. an Cox, P. 2001, MOSES 2.2 Technical Documentation, Hadley Centre Technical Report No. 30, Met Office Hadley Centre

Gregory, D. and Rowntree, P.R. 1990, A Mass Flux Convection Scheme with Representation of Cloud Ensemble Characteristics and Stability-Dependent Closure. Mon. Wea. Rev. **118** 1483-1506

Lock, A.P., Brown, A.R., Bush, M.R., Martin, G.M. and Smith, R.N.B. 2000 A New Boundary Layer Mixing Scheme. Part 1: Scheme Description and Single-Column Model Tests. *Mon. Wea. Rev.,* **128** 3187-3199

Panofsky, H. A., and G. W. Brier, 1958: Some Applications of Statistics to Meteorology. The Pennsylvania State University, 224 pp.

Stapleton, J., Wiss, V., Shanklin, D., Nguyen, T., Burgess, E., Thornton, W., Brown, T., "Radar Propagation Modeling Assessment Using Measured Refractivity and Directly Sensed Propagation Ground Truth – Wallops Island, VA 2000", NSWCDD/TR-01/132, September 2001.

Wilson, D.R., and Ballard, S.P., 1999 : A microphysically based precipitation scheme for the UK Meteorological Office Unified Model. Quart. J. Roy. Meteor. Soc., **125**, 1607-1636